


B7-H3 as a Therapeutic Target in Advanced Prostate Cancer

Journal Article

Author(s):

Guo, Christina; Figueiredo, Ines; Gurel, Bora; Neeb, Antje; Seed, George; Crespo, Mateus; Carreira, Suzanne; Rekowski, Jan; Buroni, Lorenzo; Welti, Jon; Bogdan, Denisa; Gallagher, Lewis; Sharp, Adam; Fenor de la Maza, Maria D.; Rescigno, Pasquale; Westaby, Daniel; Chandran, Khobe; Riisnaes, Ruth; Ferreira, Ana; Miranda, Susana; [Alimonti, Andrea](#)  et al.

Publication date:

2023-03

Permanent link:

<https://doi.org/10.3929/ethz-b-000604944>

Rights / license:

[Creative Commons Attribution 4.0 International](#)

Originally published in:

European Urology 83(3), <https://doi.org/10.1016/j.eururo.2022.09.004>

available at www.sciencedirect.com
journal homepage: www.europeanurology.com



Platinum Priority – Prostate Cancer

Editorial by Eugene Shenderov, Emmanuel S. Antonarakis on pp. 239–240 of this issue

B7-H3 as a Therapeutic Target in Advanced Prostate Cancer

Christina Guo^{a,b,†}, Ines Figueiredo^{a,†}, Bora Gurel^{a,†}, Antje Neeb^a, George Seed^a, Mateus Crespo^a, Suzanne Carreira^a, Jan Rekowski^a, Lorenzo Buroni^a, Jon Welti^a, Denisa Bogdan^a, Lewis Gallagher^a, Adam Sharp^{a,b}, Maria D. Fenor de la Maza^{a,b}, Pasquale Rescigno^c, Daniel Westaby^{a,b}, Khobe Chandran^{a,b}, Ruth Riisnaes^a, Ana Ferreira^a, Susana Miranda^a, Bianca Cali^d, Andrea Alimonti^{d,e,f}, Silvia Bressan^{d,g}, Alana H.T. Nguyen^h, Michael M. Shen^h, Jessica E. Hawley^{h,i}, Aleksandar Obradovic^h, Charles G. Drake^{h,j}, Claudia Bertan^a, Chloe Baker^a, Nina Tunariu^{a,b}, Wei Yuan^a, Johann S. de Bono^{a,b,*}

^aThe Institute of Cancer Research, London, UK; ^bThe Royal Marsden NHS Foundation Trust, Sutton, UK; ^cCandiolo Cancer Institute, FPO-IRCCS, Candiolo TO, Italy; ^dInstitute of Oncology Research, Oncology Institute of Southern Switzerland, Università della Svizzera Italiana, Bellinzona, Switzerland; ^eDepartment of Health Sciences and Technology, ETH Zurich, Zurich, Switzerland; ^fVeneto Institute of Molecular Medicine, Padova, Italy; ^gDepartment of Pharmaceutical and Pharmacological Sciences, University of Padova, Padova, Italy; ^hColumbia University Irving Medical Center, New York, NY, USA; ⁱUniversity of Washington, Fred Hutchinson Cancer Center, Seattle, WA, USA; ^jJanssen Research, Spring House, PA, USA

Article info

Article history:

Accepted September 2, 2022

Associate Editor:

Todd M. Morgan

Statistical Editor:

Melissa Assel

Keywords:

B7-H3
Prostate cancer
Adenocarcinoma
Neuroendocrine
DNA damage repair
Antibody drug conjugate



www.eu-acme.org/europeanurology

Please visit www.eu-acme.org/europeanurology to answer questions on-line. The EU-ACME credits will then be attributed automatically.

Abstract

Background: B7-H3 is a cell surface immunomodulatory glycoprotein overexpressed in prostate cancers (PCs). Understanding its longitudinal expression at emergence of castration resistance and association with tumour genomics are critical to the development of and patient selection for B7-H3 targeted therapies.

Objective: To characterise B7-H3 expression in same-patient hormone-sensitive (HSPC) and castration-resistant (CRPC) PC biopsies, associating this with PC genomics, and to evaluate the antitumour activity of an anti-B7-H3 antibody-drug conjugate (ADC) in human CRPC *in vitro* and *in vivo*.

Design, setting, and participants: We performed immunohistochemistry and next-generation sequencing on a cohort of 98 clinically annotated CRPC biopsies, including 72 patients who also had HSPC biopsies for analyses. We analysed two CRPC transcriptome and exome datasets, and PC scRNASeq datasets. PC organoids (patient-derived xenograft [PDX]-derived organoids [PDX-Os]) were derived from PDXs generated from human CRPC biopsies.

Outcome measurements and statistical analysis: We evaluated B7-H3 mRNA expression in relation to a panel of 770 immune-related genes, compared B7-H3 protein expression between same-patient HSPC and CRPC biopsies, determined associations with PC genomic alterations, and evaluated the antitumour activity of DS-7300a, a topoisomerase-1 inhibitor payload anti-B7-H3 ADC, in human PC cell lines, organoids (PDX-Os), and xenografts (PDXs) of different histologies, B7-H3 expressions, and genomics.

[†] These authors contributed equally to this manuscript.

* Corresponding author. The Institute of Cancer Research, Downs Road, London SM2 5PT, UK. Tel. +44 208 722 4029; Fax: +44 208 642 7979.

E-mail address: johann.de-bono@icr.ac.uk (J.S. de Bono).

<https://doi.org/10.1016/j.eururo.2022.09.004>

0302-2838/© 2022 The Author(s). Published by Elsevier B.V. on behalf of European Association of Urology. This is an open access article under the CC BY license (<http://creativecommons.org/licenses/by/4.0/>).



Results and limitations: B7-H3 was among the most highly expressed immunomodulatory genes in CRPCs. Most CRPCs (93%) expressed B7-H3, and in patients who developed CRPC, B7-H3 expression was frequently expressed at the time of HSPC diagnosis (97%). Conversion from B7-H3 positive to negative, or vice versa, during progression from HSPC to CRPC was uncommon. CRPC with neuroendocrine features were more likely to be B7-H3 negative (28%) than adenocarcinomas. B7-H3 is overexpressed in tumours with defective DNA repair gene (*ATM* and *BRCA2*) alterations and is associated with ERG expression, androgen receptor (AR) expression, and AR activity signature. DS7300a had antitumour activity against B7-H3 expressing human PC models including cell lines, PDX-Os, and PDXs of adenocarcinoma and neuroendocrine histology.

Conclusions: The frequent overexpression of B7-H3 in CRPC compared with normal tissue and other B7 family members implicates it as a highly relevant therapeutic target in these diseases. Mechanisms driving differences in B7-H3 expression across genomic subsets warrant investigation for understanding the role of B7-H3 in cancer growth and for the clinical development of B7-H3 targeted therapies.

Patient summary: B7-H3, a protein expressed on the surface of the most lethal prostate cancers, in particular those with specific mutations, can be targeted using drugs that bind B7-H3. These findings are relevant for the development of such drugs and for deciding which patients to treat with these new drugs.

© 2022 The Author(s). Published by Elsevier B.V. on behalf of European Association of Urology. This is an open access article under the CC BY license (<http://creativecommons.org/licenses/by/4.0/>).

1. Introduction

Advanced prostate cancer (PC) is a leading cause of male cancer mortality [1]. PC remains largely insensitive to current cancer immunotherapies arguably due to potent immunosuppressive mechanisms operative in this disease [2,3]. Whilst the immune checkpoint PD-L1 (B7-H1; CD274) is infrequently expressed in PC, another member of the B7 family of immunomodulatory type 1 transmembrane glycoprotein, B7-H3 (CD276), is highly expressed in PC, among other solid tumours, and is associated with worse prognosis [4–8]. Notably, B7-H3 expression has been shown to be higher in metastatic PC (mPC) than in localised PC [4,8], although inpatient comparisons of B7-H3 protein expression as PC progresses from treatment-naïve hormone-sensitive to castration-resistant metastatic disease has not been performed comprehensively. Relatively low B7-H3 expression in normal tissues, apart from the placenta, also makes B7-H3 an attractive therapeutic target [9].

Humans and other primates predominantly express the 4-immunoglobulin (Ig) form of B7-H3, comprising a tandem duplicated pair of Ig variable (IgV)-like and Ig constant (IgC)-like domains; mice express only the homologous 2Ig (IgV-IgC) protein [10]. 4-IB7-H3 has been shown to have context-dependent, pleotropic, immunomodulatory functions in autoimmunity, transplantation, and malignancy [11–18]. Studies of B7-H3 in both solid tumours and haematologic malignancies have demonstrated immune-inhibitory effects mediated by cytotoxic T cells and natural killer cells [11,14,18,19]. In contrast, in a study using the TRAMP PC mouse model (RB1 and TP53 loss of function), B7-H3 knockout generated an immunosuppressive tumour microenvironment and promoted tumour growth, although this model's predominantly neuroendocrine (NE) phenotype differs from most human prostate carcinomas [18]. Beyond its immunologic functions, B7-H3 has also been reported to increase tumour survival, stemness, chemoresistance, and metastases through modulation of pathways,

such as JAK2-STAT3, MEK, and PI3K/AKT, and anti-apoptotic proteins in models of colorectal, breast, ovarian, head and neck, and other cancers [20–22].

Several classes of B7-H3 targeted therapies, including antibody-drug conjugates (ADCs), monoclonal and bispecific antibodies, and chimeric antigen receptor (CAR)-T, are in (pre)clinical development [23–26], although none are clinically approved to date. ADCs are composed of monoclonal antibodies, joined via a linker, to a biologically active payload allowing for the delivery of potent cytotoxic directly to target-expressing cells, thereby improving the therapeutic window [27]. Trastuzumab deruxtecan (DXd), a HER2-targeting ADC with a cleavable tetrapeptide-based linker and a topoisomerase-1 (TOP1) inhibitor payload, has important antitumour activity against advanced HER2-positive breast and gastric cancer [28,29]. Targeting B7-H3 using an ADC with the same linker payload technology may be an effective strategy for treating PC.

The objectives of this study are to describe the longitudinal expression of B7-H3 in same-patient biopsies during progression from hormone-sensitive prostate cancer (HSPC) to castration-resistant prostate cancer (CRPC), to associate membranous B7-H3 (mB7-H3) expression with tumour molecular profile, and to evaluate the antitumour activity of a novel anti-B7-H3 ADC with a TOP1 inhibitor payload (DS-7300a) on human PC cell lines, patient-derived xenograft (PDX)-derived organoids (PDX-Os), and PDXs with varying levels of B7-H3 expression, histologies, and genomic backgrounds, in order to support the clinical development of effective B7-H3 targeted therapies and companion biomarkers that improve PC care.

2. Patients and methods

2.1. Patients and tissue samples

Patients with CRPC treated at the Institute of Cancer Research and Royal Marsden Hospital (ICR/RMH) between December 2011 and July 2019 were selected randomly, provided informed consent, and were enrolled onto

institutional protocols approved by the RMH ethics review committees (reference no. 04/Q0801/60). The initial analysis cohort consisted of 98 randomly selected patients ($n = 98$) with histologically confirmed formalin-fixed paraffin-embedded (FFPE) CRPC biopsies; 72/98 had diagnostic treatment-naïve HSPC biopsies. Of 98 patients, 94 had CRPC with adenocarcinoma histology and four had CRPC with adenocarcinoma histology with NE differentiation. Tumour histology was determined by board-certified pathologists. An additional cohort 18 patients treated at the ICR/RMH for CRPC with features of NE differentiation (total 22), defined by the presence of staining for CD56, chromogranin, or synaptophysin in >20% of cells, were identified to further characterise B7-H3 expression in NE PC. Clinical data were retrospectively collected from the hospital medical records ([Supplementary Fig. 1](#) and [Supplementary Tables 1 and 2](#)).

2.2. Transcriptome validation cohorts

A total of 270 metastatic CRPC (mCRPC) transcriptomes generated by the International Stand Up To Cancer/Prostate Cancer Foundation (SU2C/PCF) Prostate Cancer Dream Team [30] were downloaded and reanalysed. An independent cohort of 95 mCRPC transcriptomes from patients treated at the RMH/ICR was analysed [31].

2.3. Immunohistochemistry

Immunohistochemistry (IHC) was performed on FFPE tissue sections using an automated staining platform (Bond RX; Leica Biosystems) as described in [Supplementary Table 3](#). Bone biopsies were decalcified using pH 7 EDTA for 48 h. Antibodies against human B7-H3, ATM, MMR proteins, synaptophysin, chromogranin, CD56, RB1, p21, p16, androgen receptor (AR), AR splice variant 7 (AR-V7), PTEN, and Ki67 were validated by siRNA knockdown using Lipofectamine™ RNAiMAX Transfection Reagent (Cat 13778075; Thermo Fisher Scientific, Waltham, Massachusetts, USA) and pooled Dharmacon™ ON-TARGETplus siRNA (Horizon Discovery, Cambridge, Cambridgeshire, UK) in positive control cell lines, Western blotting, and IHC ([Supplementary material](#)) [32–35].

2.4. Genomic characterisation and mutation analyses of CRPC biopsies

CRPC biopsies were assessed for defective DNA repair (DDR) gene alterations by next-generation sequencing (NGS) using previously described methods [36]. Patients were defined as having DDR gene alterations, excluding mismatch repair defect (MMRd), based on the gene list in [Supplementary Table 4](#).

2.5. Cell line and PDX-O growth and viability assays

Human PC cells are cultured under conditions described in [Supplementary Table 5](#) and seeded in 96-well plates for drug treatment. PDX-Os were derived from PDXs generated from human CRPC biopsies using established methods described in detail in the [Supplementary material](#) [37–39]. Briefly, once organoids have formed in Matrigel matrix (Cat 356231; Corning, Tewksbury, Massachusetts, USA) domes seeded in 24-well plates, they were reseeded in 96-well plates for drug treatment. PDX-Os and PC cells were treated 1 d after reseeding with DS-7300a (anti-B7-H3 ADC), a nontargeting IgG1-ADC, the parental anti-B7-H3 antibody, the naked cytotoxic payload (DXd), or 10 mmol/l acetate buffer-5% sorbitol-pH 5.5 (ABS) vehicle (drugs and vehicle provided by Daiichi Sankyo, Tokyo, Japan). After 6 d of treatment, the viability of cell lines and PDX-Os was assessed using CellTiter-Glo 2D (Cat G9241; Promega, Madison, Wisconsin, USA) and CellTiter-Glo 3D (Cat G9681; Promega, Madison, Wisconsin, USA) viability assays, respectively. All assays were performed with three experimental and at least three technical replicates.

2.6. PDX studies

PDXs were generated from clinically annotated human CRPC biopsies using previously described methods, and characterised by IHC and whole-genome sequencing (CP50 and CP142) or targeted NGS (CP341 and CP327; [Supplementary material](#)) [37–39]. Patient tumour biopsies were also characterised by IHC and targeted NGS. Tumour-bearing mice were randomised to the following intravenous treatments: DS-7300a (3 or 10 mg/kg), nontargeting IgG1-ADC (3 or 10 mg/kg), anti-B7-H3 antibody (3 or 10 mg/kg), or ABS (3.4 ml/kg) vehicle (Daiichi Sankyo, Tokyo, Japan). Mice (four to eight per arm) were treated when tumours reached ~100 mm³, twice, 2 wk apart. Allocation was concealed from the staff administering the drugs, monitoring the mice, and measuring the tumours. Mice were weighed and monitored for distress, and tumours were measured by calliper twice per week. Mice were sacrificed and tumours were collected after 40 days from the time of treatment commencement or when tumours reached 1000 mm³, whichever occurred first.

2.7. Bioinformatics

Bulk tumour transcriptome reads were aligned to the human reference genome (GRCh37/hg19) using TopHat2 (version 2.0.7). Gene expression, as fragments per kilobase of transcript per million mapped reads, was calculated using Cufflinks [30].

Two publicly available PC single-cell RNASeq (scRNASeq) datasets from 13 HSPC and 14 CRPC patients were analysed [40,41]. Raw gene expression count matrices were downloaded from Gene Expression Omnibus (accession: GSM4203181) [41]. The R package Seurat (version 4.0.3; R Statistical Software, Vienna, Austria) [42] was used for quality control by removing cells with <1000 or >4000 distinct genes and >5% mitochondrial genes. Cells were log normalised, and dimensional reduction was performed prior to clustering. Single cells were annotated with ENCODE cell types using the SingleR (version 1.4.1) R package, using the Blueprint ENCODE data, downloaded with the celldex (version 1.0.0) R package [43] for reference. Seurat was used for dimensional reduction visualisation of cells and gene expression quantification.

2.8. Statistical analysis

All statistical analyses were performed using R Statistical Software version 4.1.3 (R Core Team, Vienna, Austria) or GraphPad Prism version 6 (GraphPad Software Inc., San Diego, California, USA), as described in the [Supplementary material](#).

3. Results

3.1. Membranous B7-H3 protein is highly expressed by advanced PC epithelial cells

To validate B7-H3 as a therapeutic target in advanced PC, we analysed two independent PC transcriptome datasets and ranked its expression in comparison with other genes in the 770-gene nCounter PanCancer Immune Profiling Panel [44], and showed that B7-H3 was among the highest expressed immune genes in the SU2C/PCF (sixth percentile) and RMH (eighth percentile) cohorts. Specifically, expression was significantly higher than that of all other members of the B7 family of immunomodulatory glycoproteins, which includes the immune checkpoints PD-L1/2 and VISTA ([Supplementary Table 6](#)) [44–47].

To characterise B7-H3 protein expression, we validated an anti-B7-H3 antibody (clone: D9M2L) against the extracellular IgV1-like domain of B7-H3 conserved across known

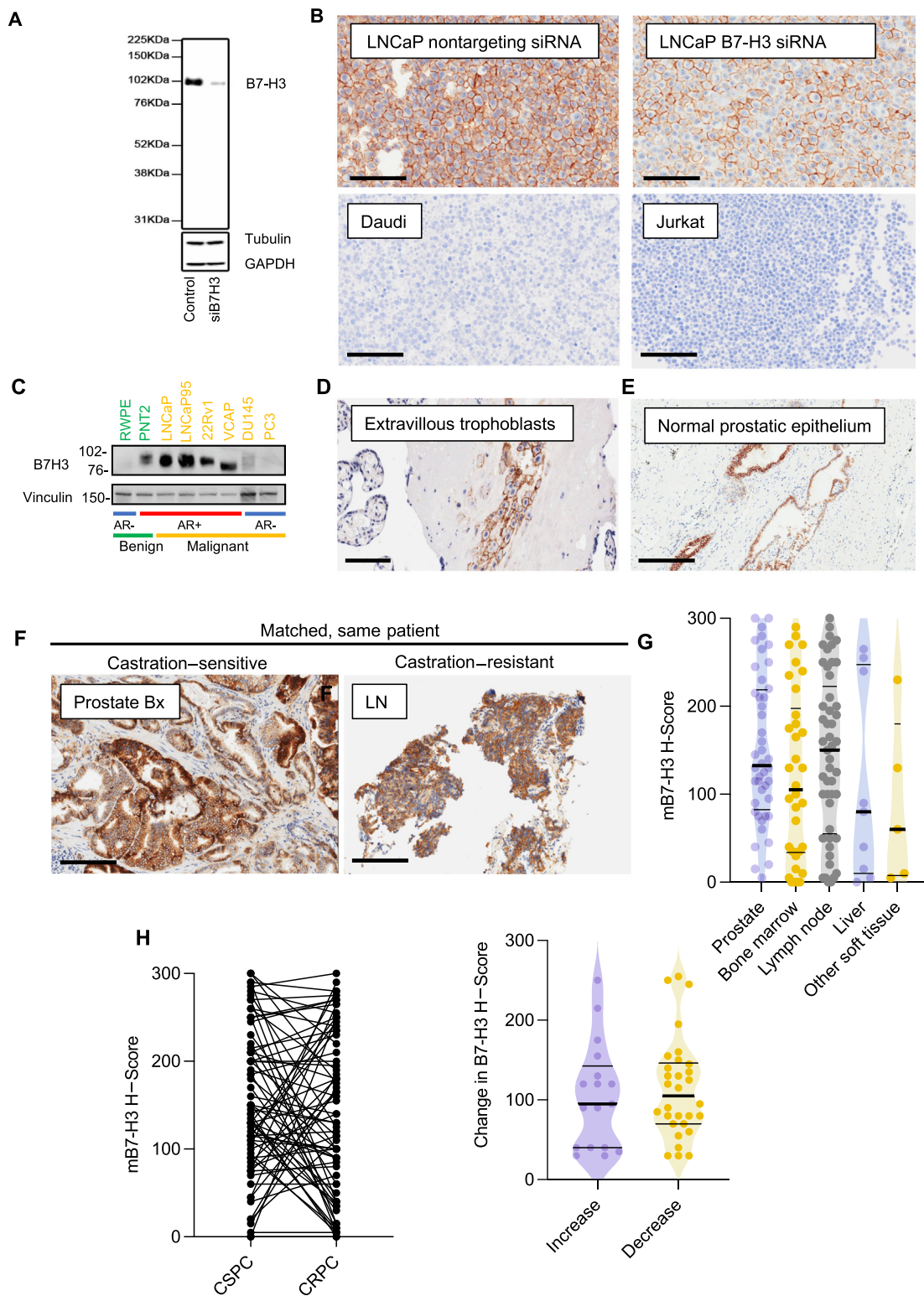


Fig. 1 – mB7-H3 protein expression in CRPC. (A) B7-H3 antibody specificity confirmed by Western blotting of whole-cell lysates from LNCaP cell line treated with non-targeting control siRNA and pooled B7-H3 siRNA. (B) IHC showing LNCaP cell pellets treated with non-targeting control siRNA or B7-H3 siRNA, Daudi cell pellets, and Jurkat cell pellets (100 µm scale bar). (C) Western blot showing B7-H3 expression in parental prostate and malignant PC cell lines. (D and E) IHC showing B7-H3 staining of extravillous trophoblasts (100 µm scale bar), and normal prostatic epithelium with preferential luminal staining and minimal basal or stromal staining (200 µm scale bar). (F) IHC showing B7-H3 staining in matched HSPC and CRPC biopsies (200 µm scale bar). (G) Expression of mB7-H3 by biopsy site. Median (IQR) for prostate: 133 (83–219); bone marrow: 105 (34–198); lymph node: 150 (55–223); liver: 249 (10–248); and soft tissue: 70 (9–232). (H) B7-H3 expression in same-patient HSPC (median: 140, IQR: 91–214) and CRPC (median: 123, IQR: 43–218) biopsies ($p = 0.25$). Kruskal-Wallis test was performed. (I) Changes in B7-H3 H score as tumours progress from HSPC to CRPC. (G–I) Horizontal bars denote interquartile ranges and medians. AR = androgen receptor; Bx = biopsy; CRPC = castration-resistant prostate cancer; HSPC = hormone-sensitive prostate cancer; IHC = immunohistochemistry; IQR = interquartile range; LN = lymph node; mB7-H3 = membranous B7-H3; PC = prostate cancer.

splice isoforms by showing a reduction in the protein expression of B7-H3 in whole-cell lysates (Western blot) and cell pellets (IHC) from LNCaP cells treated with B7-H3 siRNA. IHC of pellets from the negative control cell lines, Daudi and Jurkat, did not stain for B7-H3 (Fig. 1A and B) [10,48]. B7-H3 was expressed in AR-positive but minimally expressed by AR-negative PC cell lines, and expectedly, by extravillous trophoblasts in the human placenta, and luminal cells of benign prostatic tissue (Fig. 1C–E).

B7-H3 protein expression was evaluated in 98 mCRPC biopsies and 72 same-patient treatment-naïve HSPC biopsies. Twenty-six archival HSPCs were unavailable or of inadequate quality for IHC. Given that B7-H3 targeted therapies mostly bind membranous protein, we focused on mB7-H3, although we found a strong association between mB7-H3 and cytoplasmic B7-H3 expression ($n = 170$, Spearman's correlation [r_s] = 0.7; $p < 0.001$; Supplementary Fig. 2). Membranous B7-H3 was expressed (defined as H score [HS] ≥ 5) by the majority of CRPC (91/98 [93%]) and same-patient HSPC (70/72 [97%]) biopsies. The median mB7-H3 expression (HS) was 143 (interquartile range [IQR]: 96–214, $n = 72$) in HSPC biopsies and 128 (IQR: 40–223, $n = 98$) in CRPC biopsies.

There was no significant difference in the median mB7-H3 HS ($p = 0.1$; Fig. 1H) or in the proportion of B7-H3-positive tumours between the 72 same-patient HSPC and CRPC biopsies ($p = 1$). mB7-H3 expression changed bidirectionally across same-patient HSPC and CRPC biopsies. There was a difference in mB7-H3 HS of ≤ 30 between HSPC and CRPC biopsies in 30 patients. An increase in B7-H3 expression (>30 increase in HS) was observed in 15 patients (median increase [IQR]: 120 [40–155]), and a decrease in B7-H3 expression (>30 decrease in HS) was observed in 27 patients (median decrease [IQR]: 120 [80–150]; Fig. 1H and I). One patient with B7-H3-negative HSPC biopsy had B7-H3 staining in the CRPC biopsy, and one patient with mB7-H3 staining in the HSPC biopsies had no mB7-H3 staining in the CRPC biopsy. mB7-H3 expression between different biopsy sites was not significantly different ($p = 0.2$; Fig. 1G).

We observed intra-sample heterogeneity in mB7-H3 expression, with all B7-H3-positive biopsies also having some tumour cells with undetectable B7-H3 expression. Heterogeneity did not differ between HSPC and CRPC (median Shannon Diversity Index for HSPC: 0.98; CRPC: 1.06; $p = 0.2$; Fig. 2A). B7-H3 was primarily expressed by tumour and some endothelial cells but rarely by stromal cells (median % positive cells in tumour compartment [IQR]: 68% [40–87%]; stromal compartment: 9% [4–20%]; $p < 0.001$; Fig. 2-B and C). Membranous B7-H3-positive tumour cells were mostly within one to two cell diameters from mB7-H3-negative tumour cells (median distance [IQR]: 24 μm

[16–51 μm]; Fig. 2D). Since B7-H3 mRNA expression is positively associated with cytoplasmic and membranous protein expression, we examined immune cell B7-H3 expression using two scRNASeq datasets from 13 HSPC patients and 14 CRPC patients [40,41]. B7-H3 mRNA was predominantly expressed by tumour epithelial cells. A small subset of T cells, B cells, myelomonocytic cells, fibroblasts, natural killer cells, and endothelial cells also expressed B7-H3 mRNA (Fig. 2E–G and Supplementary Fig. 3).

3.2. Membranous CRPC B7-H3 expression and survival outcomes

Given that B7-H3 expression in diagnostic PC biopsies have been associated with PC recurrence and PC-specific mortality [4–6,49,50], we evaluated the prognostic relevance of mB7-H3. The median overall survival (OS) from the time of HSPC and CRPC biopsies was 80.7 mo (95% confidence interval [CI]: 68–106) and 49.7 wk (95% CI: 40.7–62.1), respectively. The mB7-H3 expression in mCRPC biopsies ($n = 98$) did not associate with OS from the time of mCRPC biopsy (hazard ratio [HR]: 0.93; 95% CI 0.87–1.01; $p = 0.07$), and mB7-H3 expression in the diagnostic HSPC biopsy ($n = 72$) did not associate with OS from the time of initial diagnosis (HR: 0.98; 95% CI: 0.89–1.08; $p = 0.7$). There remained no significant difference in survival outcomes when the four patients with CRPC with NE features were excluded from this analysis.

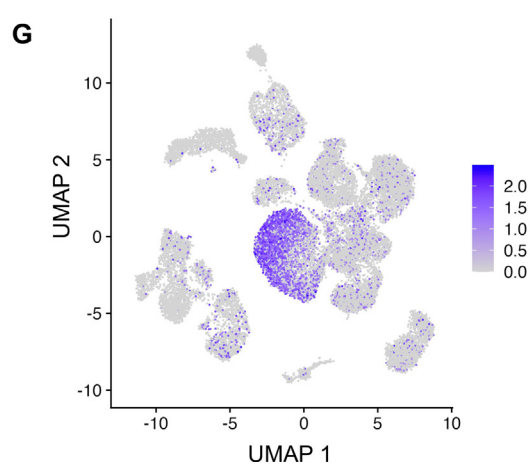
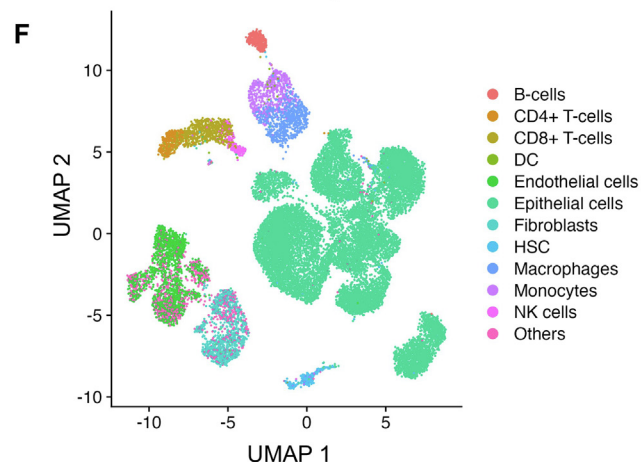
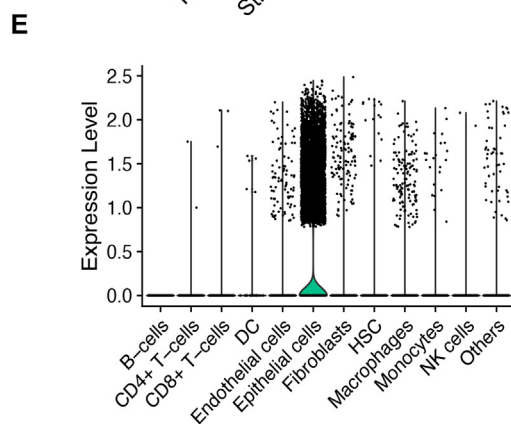
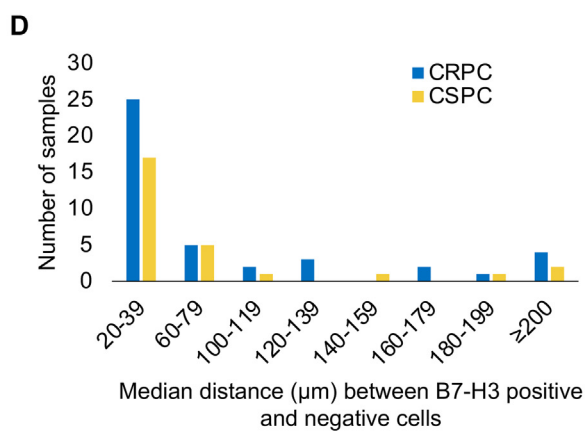
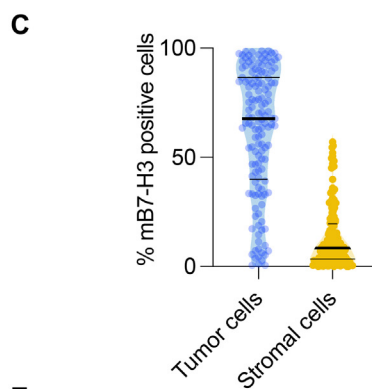
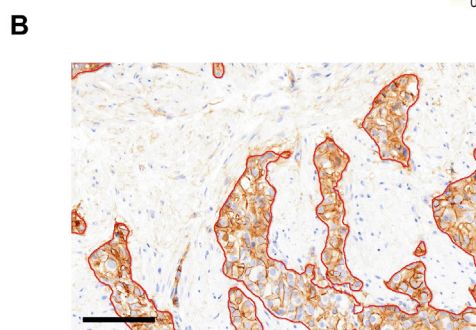
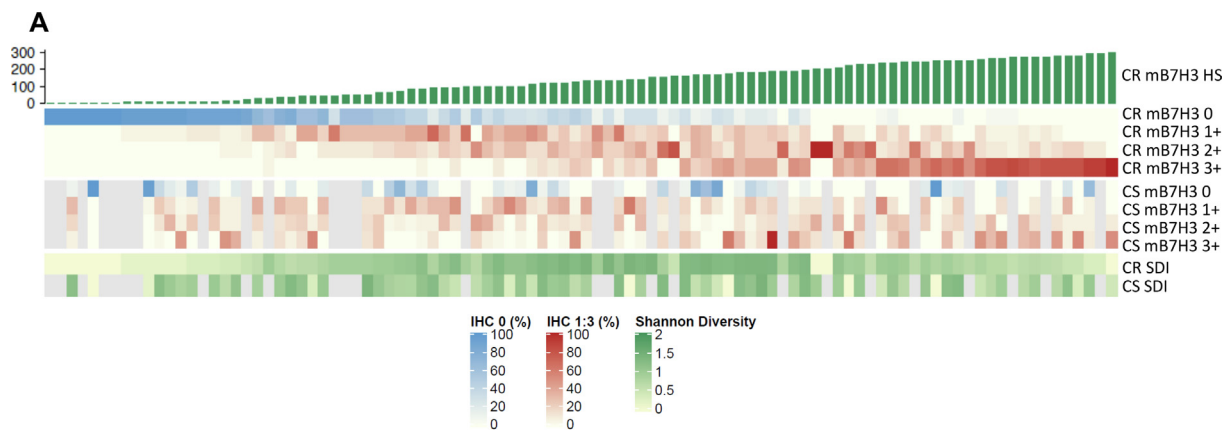
3.3. CRPC with NE features were more likely to be B7-H3 negative

Four CRPC biopsies in the initial 98-patient cohort had features of NE differentiation defined by IHC staining for synaptophysin, CD56, and/or chromogranin (Supplementary Tables 2 and 7, and Supplementary Fig. 4) [51]. To address whether B7-H3 expression differed between adenocarcinoma and NE tumours, we identified an additional 18 CRPCs with NE features. Whilst most tumours expressed mB7-H3, there were significantly more B7-H3-negative cases (mB7-H3 HS: 0) in tumours with NE features (5/22) than in those without (7/94, $p = 0.04$). In the tumours that expressed B7-H3, expression levels (median HS [IQR]: 158 [62–228]) were comparable with those of the tumours with adenocarcinoma histology.

3.4. Membranous B7-H3 expression associates with deleterious DNA damage response gene alterations, ERG expression, AR expression, and activity

Given that DNA damage and *BRCA2* depletion have been shown to upregulate the B7 family immune checkpoint, and PD-L1, and several anti-B7-H3 ADCs in development

Fig. 2 – B7-H3 is heterogeneously expressed by CSPC and CRPC. (A) Membranous B7-H3 protein expression (HS) and intrasample heterogeneity quantified by Shannon's diversity index. (B) IHC of mCRPC biopsy with tumour-stroma interface demarcated by red line (100 μm scale bar). (C) Violin plots showing the percentages of B7-H3-positive cells in the tumour and stroma of 98 mCRPC biopsies. B7-H3 was expressed in a significantly higher proportion of tumour cells (median: 67%, IQR: 40–87%) than stromal cells (median: 9%, IQR: 3–20%). Horizontal bars denote IQRs and medians. (D) Bar graph categorising HSPC and CRPC samples by the mean distance between mB7-H3-positive and mB7-H3-negative tumour cells. (E–G) The scRNASeq data from 13 HSPC biopsies with clustering by inferred cell type. (F) Corresponding UMAP of B7-H3 expression by inferred cell type clustering and (G) relative expression of B7-H3 mRNA by inferred cell type. CRPC = castration-resistant prostate cancer; CSPC = castration-sensitive prostate cancer; DC = dendritic cells; IHC = immunohistochemistry; IQR = interquartile range; HSC = hematopoietic stem cells; HS = H score; HSPC = hormone-sensitive prostate cancer; mB7-H3 = membranous B7-H3; mCRPC = metastatic castration-resistant prostate cancer; NK cells = natural killer cells; scRNASeq = single-cell RNA sequencing; UMAP = uniform manifold approximation and projection.



carry DNA damaging payloads, we evaluated for the association between B7-H3 mRNA expression and DDR gene alterations in the SU2C/PCF ($n = 270$) transcriptome dataset [36,52,53]. We showed that expression was higher in samples with DDR gene alterations involved (in)directly in homologous recombination repair than in those without ($p = 0.03$; DDR gene list in [Supplementary Tables 4 and 8](#), and [Supplementary Fig. 5](#)). In the ICR/RMH cohort, this association was not statistically significant ($n = 95$, $p = 0.07$).

We then compared mB7-H3 protein expression between mCRPC biopsies and showed that mB7-H3 expression was higher in mCRPC with DDR gene alterations, excluding MMRd ($n = 49$, median HS [IQR]: 180 [95–250]), than in tumours without the alterations ($n = 43$; median HS [IQR]: 90 [15–178]; $p < 0.001$). Specifically, higher mB7-H3 was present in tumours with biallelic *BRCA2* mutation mutations ($n = 13$, $p = 0.003$) or ATM protein loss ($n = 16$, $p = 0.02$) than in those without DDR gene alteration ([Fig. 3A–C](#)).

We also examined B7-H3 expression in relation to other common oncogenic alterations in CRPC, including *ERG* expression (surrogate for TMPRSS2-*ERG* fusion), *AR* expression and activity, *TP53* mutation/deletion, *MYC* amplification, *SPOP* mutations, and PTEN protein loss. In both the SU2C/PCF and the RMH CRPC cohort, B7-H3 mRNA expression was positively associated with *ERG* expression, *AR* expression, and an *AR* activity signature. B7-H3 protein and mRNA expression was significantly lower in the limited set of *SPOP* mutant tumours than in the set of *SPOP* wild-type tumours (mutant: $n = 5$; wild type: $n = 93$, median [IQR]: 5 [2.5–40] vs 130 [50–230], $p = 0.001$; [Fig. 3C](#) and [Supplementary Fig. 5C](#)). There was no relevant association between B7-H3 mRNA expression and *MYC* expression, B7-H3 protein expression and *TP53* mutation or deletion, or B7-H3 protein expression and PTEN protein loss (defined as cytoplasmic HS ≤ 10 ; [Fig. 3E–G](#) and [Supplementary Tables 8 and 9](#)).

3.5. Membranous B7-H3 expression and CD3⁺ tumour-infiltrating T-lymphocyte density

Given B7-H3's known immunomodulatory functions [11,12,54,55], we hypothesised that mB7-H3 expression would be associated with altered T-lymphocyte infiltration in PC. We analysed intratumoural CD3⁺ tumour-infiltrating T-lymphocyte (TIL) density by CD3 IHC in 90 of the 98 mCRPC biopsies; eight CRPC samples were excluded due to insufficient remaining tumour content. We found that mCRPC biopsies with high PC cell mB7-H3 expression, dichotomised by the median (HS ≥ 127.5), had a much lower intratumoural CD3⁺ TIL density than tumours with low mB7-H3 expression (median [IQR]: 39 [19–90] vs 104.6 [44–225] cells/mm²; $p = 0.004$; [Fig. 4A–C](#)). There was, however, no significant difference in CD3⁺ TIL density in the stromal compartment of CRPC biopsies between these tumours with B7-H3 high and low expression ($p = 0.1$). There was also no association between DDR status and intratumoural CD3⁺ TIL density.

To further delineate the relationship between PC cell mB7-H3 expression and intratumoural T-cell infiltrates, we next performed multicolour immunofluorescence on 86 mCRPC biopsies for CD4⁺, CD8⁺, CD4⁺FOXP3⁺ (regulatory),

and CD4⁺FOXP3⁻ (helper) T cells. Sixteen samples were excluded from these analyses due to insufficient tissue quantity for immunofluorescence. Membranous B7-H3 expression was positively associated with CD4⁺FOXP3⁻ cell density ($p = 0.02$). There was no association between mB7-H3 expression and CD4⁺FOXP3⁺, total CD4⁺, and total CD8⁺ T-cell density, or CD8⁺ to CD4⁺ T-cell ratio ([Fig. 4D and E](#)).

3.6. Targeting B7-H3 in patient-derived PC PDX-Os and cell lines

Next, we investigated the antitumour activity of a TOP1 inhibitor payload anti-B7-H3 ADC (DS-7300a; Daiichi Sankyo, Tokyo, Japan) [25] in B7-H3-positive and B7-H3-negative human PC cell lines and PDX-Os of adenocarcinoma (PDX-O: CP327 and CP50C; cell line: VCAP, LNCaP, and 22Rv1) and NE histology (PDX-O: CP142C; cell line: DU145 and PC3) with various genomic backgrounds ([Fig. 5A and B](#), and [Supplementary Table 10](#)) [37,38]. All patients from whom the PDX-Os were derived had progressed on standard-of-care PC treatments including taxane chemotherapy and next-generation antiandrogens ([Supplementary Fig. 6](#)). Of note, both CP50C and CP142C are B7-H3 positive and express AR-V7. CP50C also has ATM protein loss and amplification of *AR*, *AKT*, and *MYC*. CP142C harbours pathogenic *ERBB4* and *TP53* mutations, and *RB1* loss, and is synaptophysin positive. The CP327 PDX does not express B7-H3, although the CRPC tumour from which it was derived expressed low levels of mB7-H3 (HS: 10). CP327 has MMRd and mutations of *TP53*, *FANCD2*, *FANCF*, *ARID2*, and *MTOR*. In comparison with the vehicle control, parental anti-B7-H3 antibody, and nontargeting IgG1-ADC, the anti-B7-H3 ADC (DS-7300a) demonstrated significant antitumour activity in the B7-H3 positive cell lines (VCAP, LNCaP95, 22Rv1, and DU145) and PDX-Os derived from tumours with adenocarcinoma (CP50C) and adenocarcinoma with NE differentiation (CP142C) at DS-7300a concentrations of ≥ 1000 ng/ml. There was no clear association between the degree of B7-H3 positivity and tumour shrinkage, although no antitumour activity was observed in the models where B7-H3 was largely absent (PC3 and CP327C) despite these being more payload sensitive ([Fig. 5C–K](#), and [Supplementary Fig. 7](#)). In LNCaP95 and VCAP cell lines, and CP142 PDX-Os, significant antitumour activity, compared with the vehicle control and nontargeting IgG1-ADC, was also observed at a DS-7300a concentration of 500 ng/ml. CP142 PDX-O has similar B7-H3 expression to CP50C but is more sensitive to payload ([Supplementary Fig. 7B](#)). Whilst the nontargeting IgG1-ADC exhibited some nonspecific antitumour activity at the highest concentration (50 000 ng/ml), this was comparably less than that of DS-7300a, except for in 22Rv1 where tumour cell kill by the IgG1-ADC was observed at 10 000 ng/ml.

3.7. Targeting B7-H3 in mCRPC PDXs

We then evaluated the *in vivo* antitumour activity of DS-7300a, the non-targeting IgG1-ADC, and parental anti-B7-H3 antibody at 3 and 10 mg/kg, administered twice, 2 weeks apart, in three human mCRPC PDXs (CP341, CP50C, and CP327) with varying B7-H3 expression and genomic characteristics ([Fig. 5A and B](#), and [Supplementary Table 10](#)).

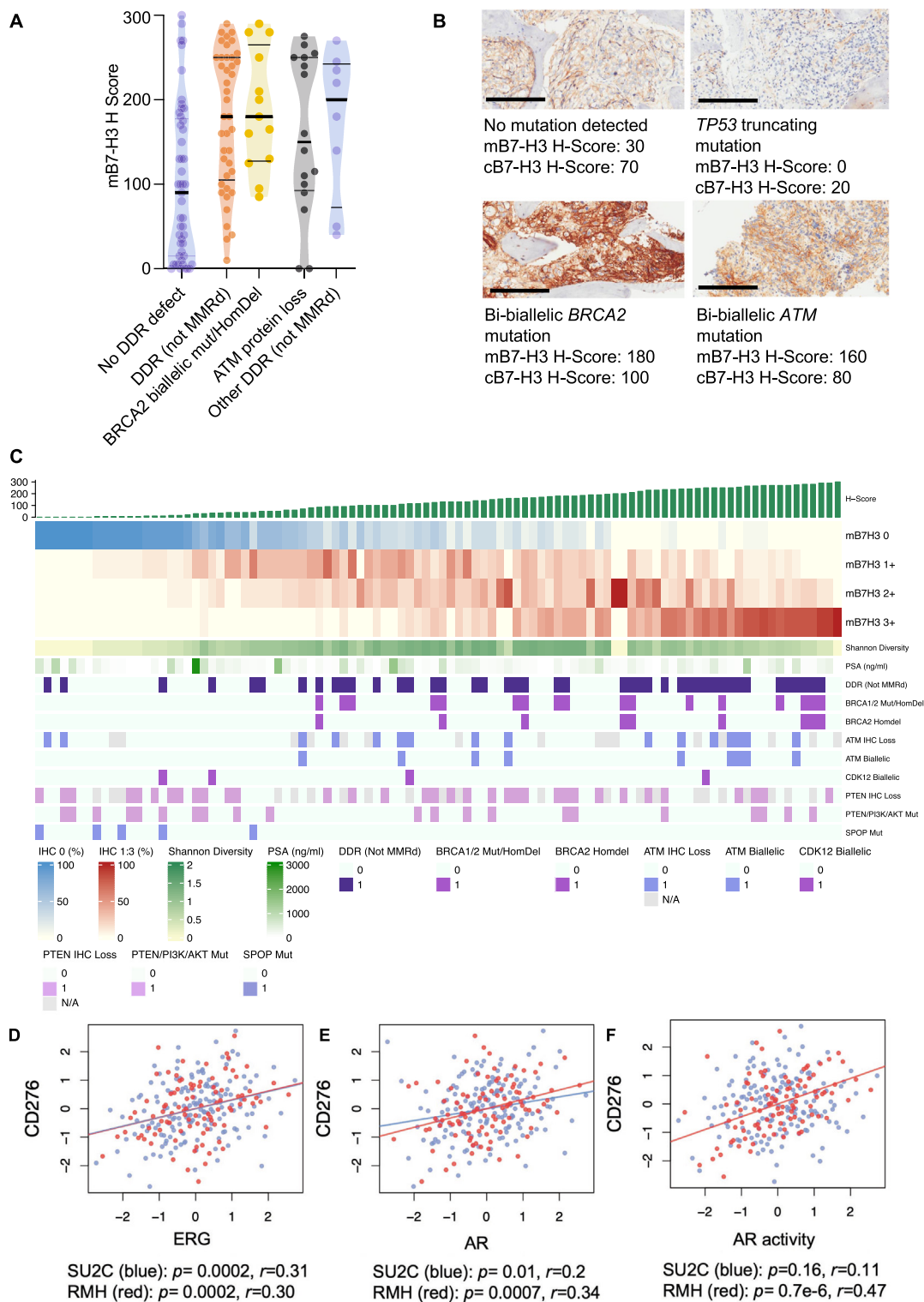


Fig. 3 – CRPC mB7-H3 expression and deleterious DDR gene alterations. (A) Expression of mB7-H3 in tumours without DDR (median: 90, IQR: 15–178, $n=43$), with DDR (median: 180, IQR: 95–250, $n=49$), *BRCA2* homozygous mutation or deletion (median: 180, IQR: 128–265, $n=13$), *ATM* protein loss (median: 150, IQR: 93–250, $n=16$), other DDR (not MMRd) (median: 200, IQR: 73–243, $n=8$). B7-H3 expression is significantly higher in tumours with DDR (excluding MMRd; $n=49$, $p=0.0001$), *BRCA2* homozygous mutation or deletion ($n=13$, $p=0.003$), and *ATM* loss ($n=16$, $p=0.02$) compared with tumours without DDR. Horizontal bars denote IQRs and medians. The p values were calculated using the Mann-Whitney U test. (B) IHC of mCRPC biopsies’ mB7-H3 expression in tumours with and without DDR gene defects (200 μm scale bar). (C) Profile of DDR gene/protein alteration and pathway alteration in 98 patients with mCRPC. Purple boxes denote the presence of alteration of the specified gene. Light blue boxes denote no detectable alteration of the specified gene. Grey boxes denote cases where IHC data were not available. (D) Association between B7-H3 (CD276) mRNA expression and ERG mRNA expression, (E) AR mRNA expression, (F) and AR activity signature. Pearson correlation coefficient (r) and p values were calculated. AR = androgen receptor; cB7-H3 = cytoplasmic B7-H3; CRPC = castration-resistant prostate cancer; DDR = DNA damage repair; HomDel = homozygous deletion; IHC = immunohistochemistry; IQR = interquartile range; mB7-H3 = membranous B7-H3; MMRd = mismatch repair defect; Mut = mutation; N/A = not available; PSA = prostate-specific antigen; RMH = Royal Marsden Hospital; SU2C = International Stand Up To Cancer; WT = wild type.

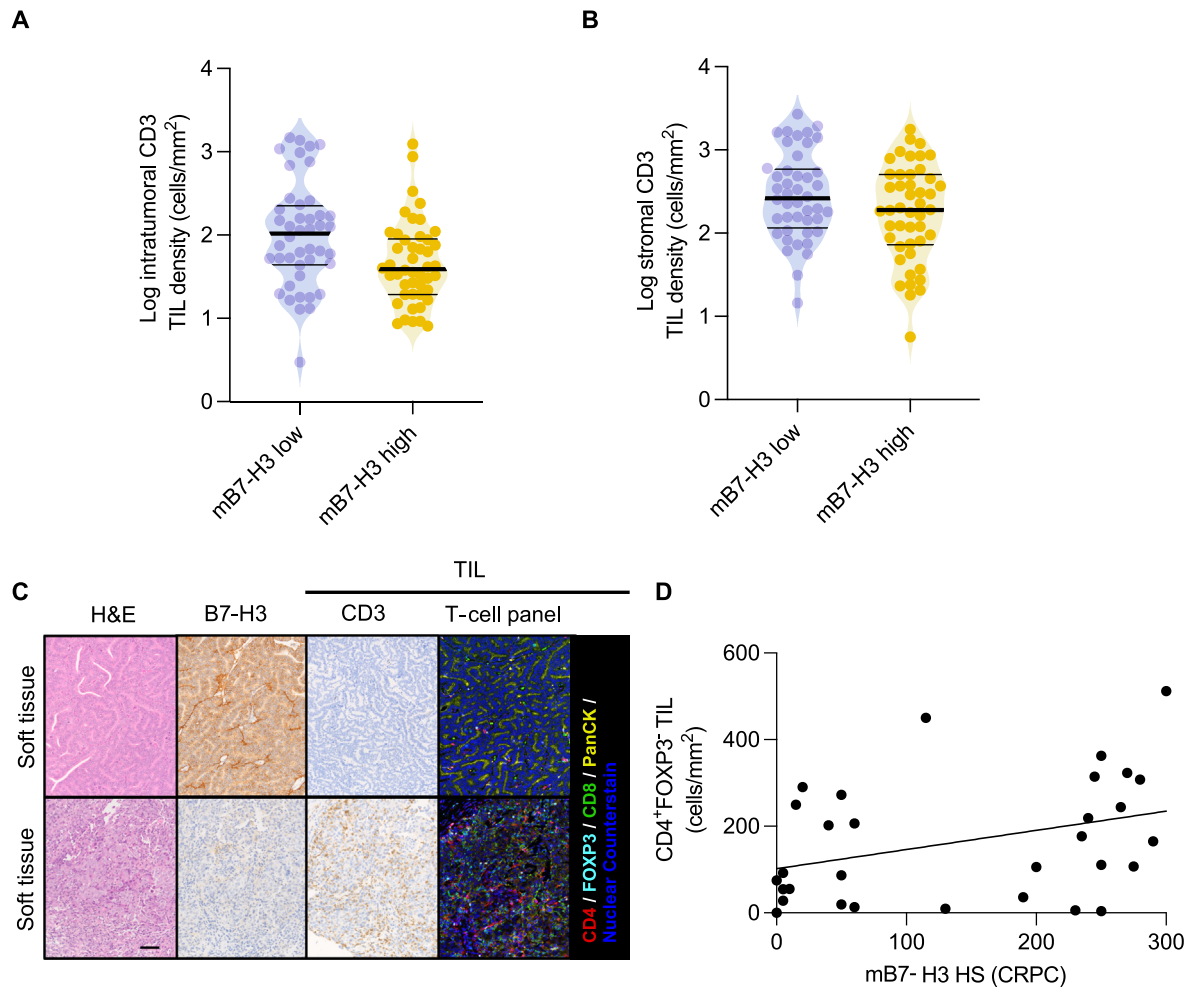
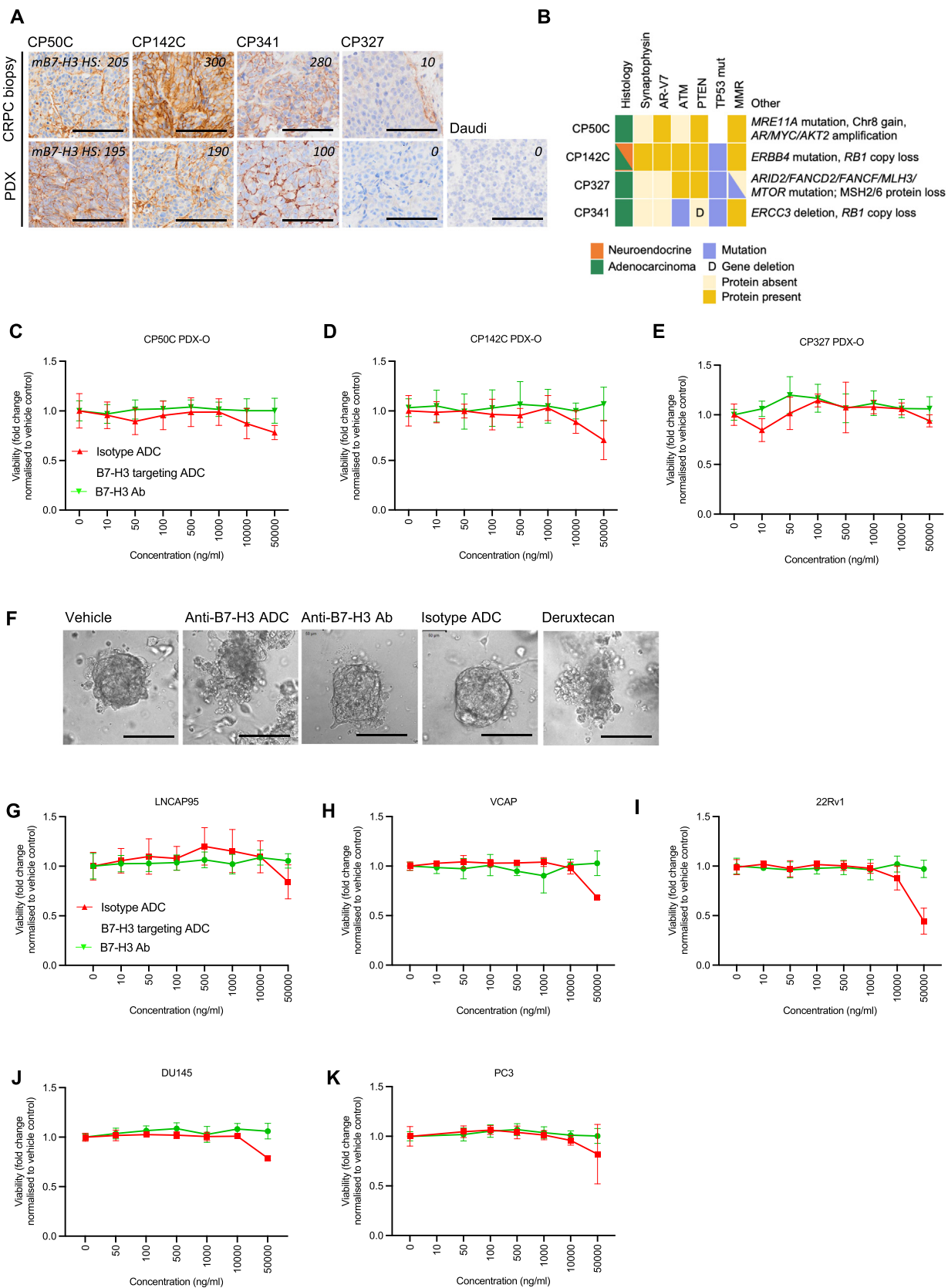


Fig. 4 – CRPC mB7-H3 associated with lower intratumoural CD3⁺ TIL density. (A) Intratumoural CD3⁺ TIL density in mB7-H3 low (HS <127.5 [median]) versus mB7-H3 high tumours (HS ≥127.5). Median (IQR): 105 cells/mm² (44–225 cells/mm²) in B7-H3 low tumour versus 39 cells/mm² (19–90 cells/mm²) in B7-H3 high tumour ($p = 0.004$). (B) Stromal CD3⁺ TIL density. Median (IQR): 263 cells/mm² (116–590 cells/mm²) in B7-H3 low tumour versus 190 cells/mm² (73–506 cells/mm²) in B7-H3 high tumour ($p = 0.1$). Horizontal bars denote median and IQR. The p values were calculated using the Mann-Whitney U test. (C) Immunohistochemistry for B7-H3 and CD3 in tumours with B7-H3 high and low expression (100 μ m scale bar). A scatter plot showing associations between tumour epithelial mB7-H3 expression and intratumoural (D) CD4⁺FOXP3⁻ and (E) CD4⁺FOXP3⁺ cell densities. Associations were determined by Spearman's rank correlations. CRPC = castration-resistant prostate cancer; HS = H score; IQR = interquartile range; mB7-H3 = membranous B7-H3; TIL = tumour-infiltrating T lymphocyte.

DS-7300a demonstrated potent, dose-dependent antitumour activity compared with vehicle, the anti-B7-H3 antibody, and the non-targeting IgG1-ADC in both B7-H3 positive PDXs (CP341 and CP50C) but not in the B7-H3 negative PDX (CP327C) despite it being more payload sensitive when grown as PDX-Os *in vitro* (Supplementary Fig. 7). Growth retardation was observed in CP50C PDXs. In CP341 PDXs, we observed tumour regression, including complete tumour responses at the 10 mg/kg dose (Fig. 6, and Supplementary Figs. 8 and 9). We did not observe associations between mB7-H3 expression and response to DS-7300a among the B7-H3-positive tumours. Although mB7-H3 expression was lower in CP341 PDXs than in the ATM-loss CP50C PDX, the CP341 CRPC tumour also harboured pathogenic *ATM* and *TP53* mutations as well as *RB1* copy loss and *ERCC3* deletion. The patient from which CP341 tumours were derived subsequently had partial radiologic and biochemical response to epirubicin, carboplatin,

and 5-fluorouracil, suggesting the presence of replication stress. Mice did not lose weight or become moribund in the context of any treatment.

Pharmacodynamic analyses of end-of-treatment CP50C and CP341 tumours confirmed the anti-proliferative effect of DS-7300a shown by a marked reduction in Ki67 in PDX-Os treated with DS-7300a (10 mg/kg) compared with the vehicle, non-targeting IgG1-ADC, and anti-B7-H3 antibody at corresponding concentrations. In both models, DS-7300a treated PDX tumours exhibited morphologic features of senescence, characterised by the flattening and enlargement of the cells, irregular and enlarged nuclei, and vacuolisation. This was also associated with an increase in staining for the senescence markers SA- β -galactosidase and p21. Both models had post-transcriptional p16 loss. Interestingly, in both responding models, post-treatment tumour B7-H3 expression was similar to that of the parental PDX tumours and did not differ across the treatment arms,



indicating the presence of potential B7-H3 expression independent resistance mechanisms (Fig. 6G and H, and Supplementary Fig. 9).

4. Discussion

B7-H3 is one of the most highly expressed immunomodulatory molecules in PC, with numerous B7-H3 targeted therapies currently in clinical development. To our knowledge, this is the first study to characterise B7-H3 protein expression during progression from HSPC to CRPC in matched, same-patient biopsies and to identify the association between B7-H3 expression and DDR gene alterations in PC. In light of this, we evaluated the antitumour activity of DS-7300a, an anti-B7-H3 ADC with a TOP1 inhibitor (DXd) payload, and demonstrated B7-H3-dependent antitumour activity in human advanced PC models *in vitro* and *in vivo*.

We showed that B7-H3 is expressed in the vast majority of patients with mCRPC, including tumours with NE features, although NE phenotype tumours were more likely to have B7-H3 protein loss. We also confirmed the association between B7-H3 expression and AR activity since B7-H3 was consistently expressed by AR-positive PC cell lines and was low or absent in AR-negative cell lines, associated with ERG expression, AR expression, and activity. These findings are consistent with previous reports showing that B7-H3 expression was more intense and frequent in mPC than in localised PC, commonly expressed by circulating tumour cells from patients with mPC (80–90% of patients), and was associated with an AR signature positive, NE signature negative PC phenotype [8,56,57]. AR has been implicated as a transcriptional regulator of B7-H3 [4].

B7-H3 expression in primary prostatectomy samples has previously been shown to be associated with increased rates of PC recurrence and PC-specific death [4–6,49,50,57], although there is conflicting evidence as to whether B7-H3 is prognostic for survival independently of tumour grade and stage [4,6]. We did not observe any association of mB7-H3 expression in HSPC and CRPC biopsies with survival; however, this may be due to the majority of

patients in this cohort having high-risk, metastatic disease and some level of B7-H3 expression. Further, a comparison of same-patient HSPC and CRPC biopsies revealed no significant difference in the median B7-H3 expression between HSPC and CRPC, suggesting that in tumours with aggressive biology and metastatic potential, B7-H3 upregulation already occurred early by the time of diagnosis. Indeed, B7-H3 overexpression has been shown in preclinical models to promote tumour metastases and invasion in multiple tumour types [58]. The lack of switch in B7-H3 positivity between HSPC and CRPC is also relevant for biomarker development for B7-H3 targeting, since if the threshold of target expression necessary for response is low, biomarker analyses could be performed on archival tissue, thereby sparing patients from invasive, fresh CRPC tumour biopsies. Whilst we observed intratumoural heterogeneity in B7-H3 expression, the close proximity between B7-H3 positive and B7-H3 negative cells bears relevance for the clinical development of anti-B7-H3 ADCs—particularly those with permeable payloads such as DS-7300a—that could engage in bystander kill [27,59].

We orthogonally demonstrated using independent CRPC cohorts that B7-H3 expression was associated with homologous recombination repair defects (HRDs), suggesting a link between expression and DNA double-strand breaks and repair. Cancers with genomic instability induced by microsatellite instability, HRD, chemotherapy, or radiation have been reported to upregulate other B7 family members, such as PD-L1, through JAK-STAT-IRF1 signalling, and sensitise to PD-L1 targeted therapies [52,60,61]. Whilst PD-L1 is expressed in less than a quarter of PC cases [7,62], B7-H3 overexpression specifically in HRD tumours is in keeping with the evidence that tumours with DDR can activate specific immune evasive mechanisms [32,63], and supports further mechanistic studies of B7-H3 modulation and rational combination therapeutics targeting B7-H3 in these PC genomic subsets. In contrast to a previous study that showed that B7-H3 was marginally higher in tumours with PTEN loss, we did not observe significant associations between B7-H3 expression and PTEN status. Notably, in our study, a more stringent cut-off for defining PTEN loss

Fig. 5 – Anti-B7-H3 ADC with a TOP1 inhibitor payload has antitumour activity in human CRPC models *in vitro*. (A) B7-H3 IHC in tumour biopsies and corresponding PDXs used for *in vivo* drug studies and from which PDX-Os were generated for *in vitro* drug studies. IHC of Daudi cell pellet was negative control (100 μ m scale bar). (B) Molecular characteristics of PDX models used for B7-H3 drug studies. (C–E) B7-H3-positive (CP50C and CP142C) and B7-H3-negative (CP327) human CRPC PDX-Os were treated with DS-7300a (anti-B7-H3 ADC), parental anti-B7-H3 antibody, nontargeting IgG1-ADC, or DXd. Viability was significantly different between treatment arms for the CP50C ($p < 0.001$) and CP142 ($p < 0.001$) models, but not for the CP327 model. Viability was significantly lower in CP50C PDX-Os treated with the anti-B7-H3 ADC than in those treated with the nontargeting IgG1-ADC at 1000, 10 000, and 50 000 ng/ml (all $p < 0.001$). Viability was significantly lower in the CP142C PDX-Os treated with the anti-B7-H3 ADC than in those treated with the nontargeting IgG1-ADC at drug concentrations of 1000, 10 000, and 50 000 ng/ml (all $p < 0.001$). (F) Confocal imaging showing CP50C PDX-Os after 6 days of treatment with the anti-B7-H3 ADC, parental anti-B7-H3 antibody, nontargeting IgG1-ADC, or DXd payload (100 μ m scale bar). (G–K) B7-H3 positive and B7-H3 negative PC cell lines were treated with DS-7300a (anti-B7-H3 ADC), parental anti-B7-H3 antibody, nontargeting IgG1-ADC, DXd payload, or vehicle. Significant differences in ($p < 0.001$) in cell viability were observed between the different treatment arms in LNCaP95 (500, 1000, 10 000, and 50 000 ng/ml), VCAP (500, 1000, 10 000, and 50 000 ng/ml), 22Rv1 (10 000 and 50 000 ng/ml), and DU145 (10 000 and 50 000 ng/ml) prostate cancer cell lines. Cell viability was significantly lower in cells treated with anti-B7-H3 ADC than in those treated with the nontargeting IgG1-ADC at these concentrations in LNCaP, VCAP, and DU145 cells (all $p < 0.001$). Cell viability was significantly lower in cells treated with anti-B7-H3 ADC than in those treated with the parental anti-B7-H3 antibody at these concentrations in LNCaP, VCAP, 22RV1, and DU145 cells (all $p < 0.001$). For all viability experiments (C–E and G–K), the mean viability and standard deviation from three individual experiments with at least three technical replicates per experiment are shown. Viability was determined using CellTiter-Glo two- or three-dimensional viability assay after 6 days. The p values for comparisons across all three treatment groups were calculated by one-way ANOVA and p values for comparisons between two treatment arms were calculated using unpaired Student t test. Ab = antibody; ADC = antibody-drug conjugate; ANOVA = analysis of variance; CRPC = castration-resistant prostate cancer; DXd = deruxtecan; Ig = immunoglobulin; IHC = immunohistochemistry; PC = prostate cancer; PDX = patient-derived xenograft; PDX-O = PDX-derived organoid; TOP1 = topoisomerase-1.

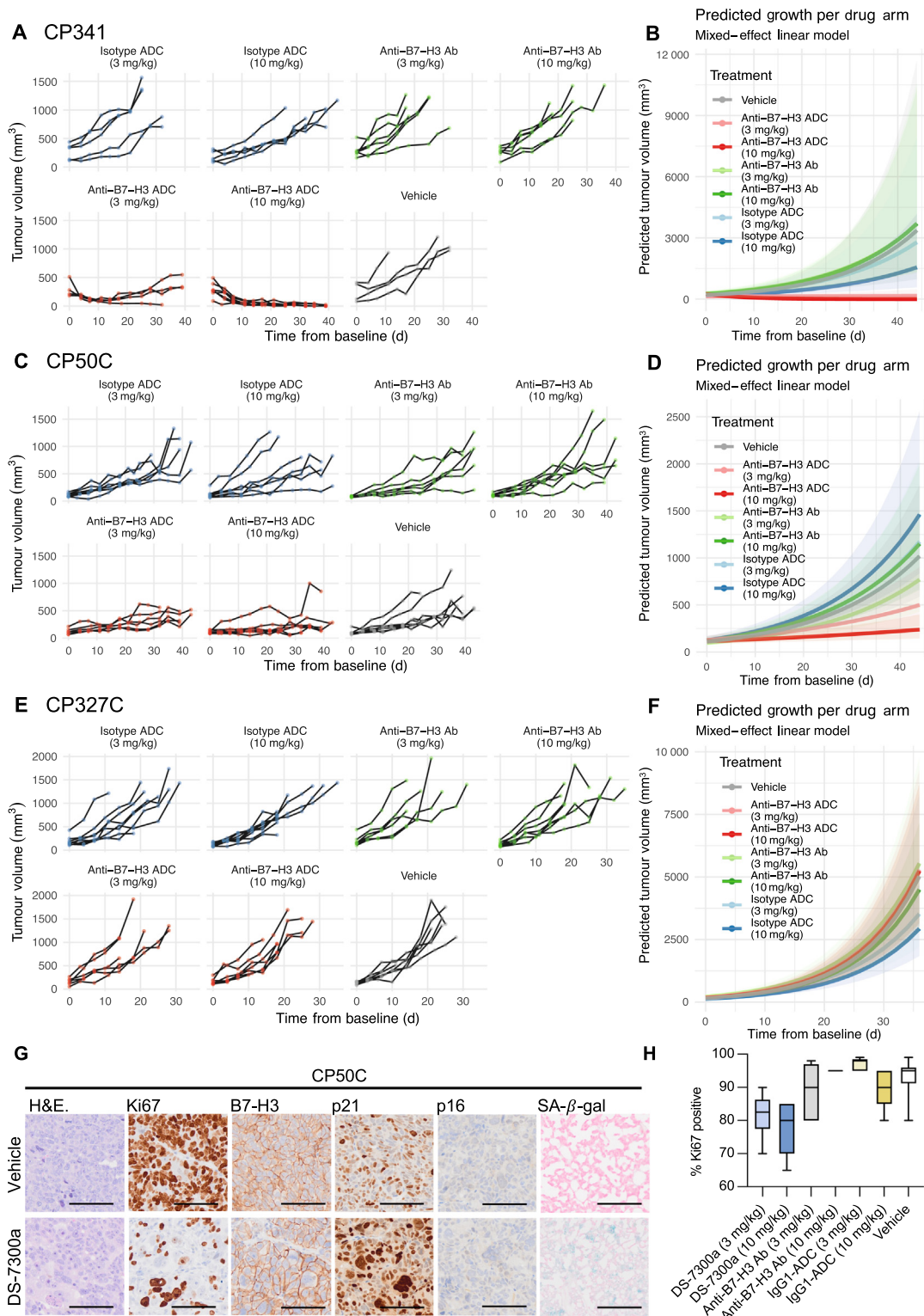


Fig. 6 – Anti-B7-H3 ADC with a TOP1 inhibitor payload has antitumour activity in human CRPC models *in vivo*. (A, C, and E) Individual tumour volumes of CP341, CP50C, and CP327 PDX models over time in PDXs treated with DS-7300a (anti-B7-H3 ADC), parental anti-B7-H3 antibody, nontargeting IgG1-ADC, or vehicle (3.4 ml/kg). (B, D, and F) Predicted tumour growth using a linear mixed-effect model of CP341, CP50C, and CP327 PDXs treated with DS-7300a (anti-B7-H3 ADC), anti-B7-H3 antibody, nontargeting IgG1-ADC, or ABS vehicle. (G) Representative IHC and SA-β-galactosidase staining of end-of-treatment CP50C tumours from mice treated with vehicle control or DS-7300a (100 μm scale bar). (H) Ki67 expression (% positive cells) in end-of-treatment CP50C tumours. Tumour Ki67 was significantly lower in mice treated with anti-B7-H3 ADC (10 mg/kg) than in those treated with nontargeting IgG1-ADC (10 mg/kg, $p < 0.001$), anti-B7-H3 antibody (10 mg/kg, $p < 0.001$), and vehicle ($p < 0.001$). Tumour Ki67 in mice treated with DS-7300a (3 mg/kg) was significantly lower than in those treated with nontargeting IgG1-ADC (3 mg/kg, $p < 0.001$) and vehicle ($p < 0.001$). Bars represent maximum and minimums, interquartile ranges, and median. The p values were calculated using the unpaired Student t test. Ab = antibody; ABS = acetate buffer-5% sorbitol-pH 5.5; ADC = antibody-drug conjugate; CRPC = castration-resistant prostate cancer; Ig = immunoglobulin; IHC = immunohistochemistry; PDX = patient-derived xenograft; TOP1 = topoisomerase-1.

was used, the sample size was smaller, and the PTEN intact arm had a relatively high proportion of tumours with DDR gene alterations [64].

Whilst tumour expression of B7-H3 can be exploited for B7-H3 targeted therapies, we also explored the potential immunologic effect of B7-H3. We show that CD3⁺ TIL density is lower in tumours with high B7-H3 expression, despite *BRCA2*-mutant PC previously being reported in a case series to have higher CD4⁺ T-cell infiltrate than *BRCA2* wild-type PC, although this relationship was not observed in our cohort [63]. This is in keeping with the immunosuppressive role of B7-H3 in CD4 and CD8⁺ T-cell responses in preclinical models of malignancy and autoimmunity [13,15,16]; coculture experiments of B7-H3 expressing and nonexpressing antigen-presenting cells in combination with alloreactive T cells also showed that B7-H3 can inhibit the proliferation of T cells [16].

Given that B7-H3 is often overexpressed in mCRPC, particularly in those with HRDs, we evaluated the antitumour activity of DS-7300a, a TOP1 inhibitor payload anti-B7-H3 ADC in tumours with varying levels of B7-H3 expression and genomic backgrounds including HRDs. We showed dose-dependent cytotoxicity *in vitro* and *in vivo* in tumours with NE differentiation and adenocarcinomas. Consistent with clinical studies of other DXd-payload ADCs, we showed that target expression was necessary for response, but additional factors clearly impacted this [65,66] given the differences in response in tumours with similar B7-H3 expression and the observation that tumour cells remaining after DS-7300a treatment in B7-H3-positive PDX models had comparable B7-H3 expression compared with parental tumour and control drug-treated tumours.

The response to ADCs depends on the complex interplay of multiple factors including target expression and turnover, ADC stability, drug-stromal interactions, drug internalisation, processing, degradation, efflux, tumour genomic background, and payload sensitivity [27]. Interestingly, CP341 (*RB1* copy loss, *ATM/ERCC3/TP53* mutant, and adenocarcinoma) PDX-Os were more sensitive to DS-7300a than CP50C (*ATM* loss and adenocarcinoma) despite having lower target expression. TOP1 inhibitors cause replication stress and tumour cell kill by trapping TOP cleavage complexes, which leads to blocking of DNA religation, and generation of single- and subsequently double-strand breaks [67]. The combination of deleterious alterations of *ATM*, involved in sensing DNA damage and initiating DDR; *RB1*, involved in DSB repair by canonical non-homologous end joining; and *ERCC3*, involved in nucleotide excision repair has been shown to confer synthetic lethality with and sensitise to TOP1 inhibition [67–69].

In vivo tumour models that responded to DS-7300a showed morphologic features of senescence, downregulated Ki67, and upregulated SA- β -galactosidase and p21. p16 has been shown to be upregulated at later stages of senescence and is important for the maintenance of senescence after cell cycle arrest is first triggered by p21 signalling in fibroblast models; therefore, these PC models' post-transcriptional loss of p16 protein led us to posit senescence reversal as a potential resistance mechanism [70]. Overall, our results indicate that whilst B7-H3 expres-

sion is necessary for response, the level of expression did not correlate with response, and therefore patient selection for B7-H3 targeting needs to consider additional factors such as alterations of DDR genes, *RB1*, *TP53*, cell cycle, and senescence regulation. Elucidating these factors may also guide dose-finding decisions during ADC development that can be personalised for specific PC subsets.

Limitations of this study are as follows. We showed an association between B7-H3 expression and DDR gene defects, but causality and mechanisms through which DDR impacts B7-H3 expression is beyond the scope of this report. We do not address inter-metastasis heterogeneity. Clinical correlations may be underpowered to detect small differences in survival, particularly in a cohort where the majority of patients had tumours expressing B7-H3 and all patients had metastatic disease. We used immunodeficient human CRPC PDXs because the antitumour activity from DS-7300a is primarily from its cytotoxic effect; however, the immunologic impact of DS-7300a cannot be addressed adequately. On-target, off-tumour toxicity may not be observed in PDXs expressing mouse 2-Ig-B7-H3 outside of the tumour. Analyses of potential biomarkers of response to DS-7300a are hypothesis generating given the small number of models studied and require interrogation in adequately powered, prospective, clinical cohorts.

5. Conclusions

In summary, we show that B7-H3, a druggable member of the B7 family of immune-modulatory glycoproteins, is associated with DDR gene defects, including deleterious *BRCA2* and *ATM* alterations in PC. B7-H3 targeting using an anti-B7-H3 ADC with a TOP1 inhibitor payload has antitumour activity in B7-H3 expressing PC *in vitro* and *in vivo*. Molecular characteristics impacting DDR and replication stress need to be interrogated as part of a biomarker suite for this therapy. Clinical trials evaluating DS-7300a in solid tumours are on-going (NCT04145622, NCT05280470).

Author contributions: Johann S. de Bono had full access to all the data in the study and takes responsibility for the integrity of the data and the accuracy of the data analysis.

Study concept and design: Guo, Figueiredo, Gurel, de Bono.

Acquisition of data: Guo, Figueiredo, Gurel, Crespo, Carreira, Welti, Buroni, Neeb, Westaby, Chandran, Rescigno, Gallagher, Fenor de la Maza, Riisnaes, Ferreira, Mirada, Cali, Bressan, Baker, Bertan, Tunariu, Yuan, Nguyen, Obradovic.

Analysis and interpretation of data: Guo, Figueiredo, Gurel, Carreira, Rekowski, Seed, Yuan, Bogdan.

Drafting of the manuscript: Guo, Figueiredo, de Bono.

Critical revision of the manuscript for important intellectual content: Guo, Figueiredo, Gurel, Carreira, Rekowski, Sharp, Seed, Cali, Alimonti, Shen, Nguyen, Hawley, Drake, de Bono, Neeb.

Statistical analysis: Guo, Rekowski, Seed.

Obtaining funding: de Bono, Guo, Shen, Drake.

Administrative, technical, or material support: None.

Supervision: de Bono, Sharp, Shen.

Other: None.

Financial disclosures: Johann S. de Bono certifies that all conflicts of interest, including specific financial interests and relationships and affiliations relevant to the subject matter or materials discussed in the manuscript (eg, employment/affiliation, grants or funding, consultancies, honoraria, stock ownership or options, expert testimony, royalties, or patents filed, received, or pending), are the following: J.S. de Bono, C. Guo, A. I. Figueiredo, B. Gurel, M. Crespo, S. Carreira, J. Rekowski, A. Neeb, J. Welti, A. Sharp, M. Fenor de la Maza, D. Westaby, G. Seed, K. Chandran, L. Buroni, L. Gallagher, D. Bogdan, R. Riisnaes, A. Ferreira, S., Miranda, C. Baker, Claudia Bertan, L. Buroni, and W. Yuan are employees of The ICR, which has a commercial interest in abiraterone, PARP inhibition in DNA repair defective cancers, and PI3K/AKT pathway inhibitors. J.S. de Bono has served on advisory boards and received fees from companies including Amgen, Astra Zeneca, Astellas, Bayer, Bioxel Therapeutics, Boehringer Ingelheim, Cellcentric, Daiichi, Eisai, Genentech/Roche, Genmab, GSK, Harpoon, Janssen, Merck Serono, Merck Sharp & Dohme, Menarini/Silicon Biosystems, Orion, Pfizer, Qiagen, Sanofi Aventis, Sierra Oncology, Taiho, Terumo, and Vertex Pharmaceuticals; reports research funding from Daiichi Sankyo for other research projects; has funding or other support for his research work from Daiichi Sankyo, Astra Zeneca, Astellas, Bayer, Cellcentric, Daiichi, Genentech, Genmab, GSK, Janssen, Merck Serono, MSD, Menarini/Silicon Biosystems, Orion, Sanofi Aventis, Sierra Oncology, Taiho, Pfizer, and Vertex; was named as an inventor, with no financial interest, for patent 8,822,438; has been the CI/PI of many industry-sponsored clinical trials; and is a National Institute for Health Research (NIHR) Senior Investigator. A. Sharp has received travel support from Sanofi (2015) and Roche-Genentech (2017 and 2019), and speaker honoraria from Astellas Pharma (2018). P. Rescigno served on the advisory boards of MSD and AstraZeneca, Italy. J.E. Hawley has served as a paid consultant to Seagen and has received sponsored research funding to her institution from Regeneron and Dendreon. C.G. Drake is an employee of Janssen Research.

Funding/Support and role of the sponsor: The de Bono, Shen, and Alimonti laboratories acknowledge research funding from the United States Department of Defense (W81XWH2110076). The de Bono laboratory acknowledges funding from the Prostate Cancer Foundation, Cancer Research UK, Prostate Cancer UK, the Movember Foundation through the London Movember Centre Of Excellence (CE013_2-002), The V Foundation for Cancer Research (D2016-022), and the UK Department of Health through an Experimental Cancer Medicine Centre (ECMC) grant. The views expressed in this article are those of the author(s) and not necessarily those of the National Health Services, the NIHR, or the Department of Health. C. Guo is supported by the Wellcome Trust. D. Westaby is supported by Cancer Research UK. P. Rescigno is supported by Prostate Cancer Foundation through a PCF YI award, and by the PTC RC SEE PROS ONCOLOGIA-FPRC 5 PER MILLE-MS 2017. A. Sharp has been supported by the Medical Research Council (MR/M018318/1), the Academy of Medical Sciences (SGL014\1015), Prostate Cancer UK (AMS15-001), and is currently supported by the Prostate Cancer Foundation (18YOUN25) and Wellcome Trust (219594/Z/19/Z). Alimonti laboratory acknowledges funding from the Swiss Cancer League (#5262), SNSF (#310030B_201274/1), Novartis Foundation, PCF (#19CHAL08), ISREC Foundation, Fondazione San Salvatore, AIRC (#22030), and the European Research Council (CoG #683136). Daiichi Sankyo approved the manuscript.

Acknowledgements: The authors thank Yui Tanaka, Nanae Izumi, Max Qian, and the Daiichi Sankyo team. Daiichi Sankyo provided DS7300a, its parental anti-B7-H3 antibody, and the isotype non-targeting IgG1-ADC. No funding or financial support was provided by Daiichi Sankyo for this project.

Peer Review Summary

Peer Review Summary and Supplementary data to this article can be found online at <https://doi.org/10.1016/j.eururo.2022.09.004>.

References

- [1] Sartor O, de Bono JS. Metastatic prostate cancer. *N Engl J Med* 2018;378:1653–4.
- [2] Kwon ED, Drake CG, Scher HI, et al. Ipilimumab versus placebo after radiotherapy in patients with metastatic castration-resistant prostate cancer that had progressed after docetaxel chemotherapy (CA184-043): a multicentre, randomised, double-blind, phase 3 trial. *Lancet Oncol* 2014;15:700–12.
- [3] de Bono JS, Guo C, Gurel B, et al. Prostate carcinogenesis: inflammatory storms. *Nat Rev Cancer* 2020;20:455–69.
- [4] Benzon B, Zhao SG, Haffner MC, et al. Correlation of B7–H3 with androgen receptor, immune pathways and poor outcome in prostate cancer: an expression-based analysis. *Prostate Cancer Prostatic Dis* 2017;20:28–35.
- [5] Roth TJ, Sheinin Y, Lohse CM, et al. B7–H3 ligand expression by prostate cancer: a novel marker of prognosis and potential target for therapy. *Cancer Res* 2007;67:7893–900.
- [6] Zang X, Thompson RH, Al-Ahmadie HA, et al. B7–H3 and B7x are highly expressed in human prostate cancer and associated with disease spread and poor outcome. *Proc Natl Acad Sci U S A* 2007;104:19458–63.
- [7] Haffner MC, Guner G, Taheri D, et al. Comprehensive evaluation of programmed death-ligand 1 expression in primary and metastatic prostate cancer. *Am J Pathol* 2018;188:1478–85.
- [8] Zhang T, Agarwal A, Almquist RG, et al. Expression of immune checkpoints on circulating tumor cells in men with metastatic prostate cancer. *Biomarker Res* 2021;9:14.
- [9] Petroff MG, Kharatyan E, Torry DS, Holets L. The immunomodulatory proteins B7–DC, B7–H2, and B7–H3 are differentially expressed across gestation in the human placenta. *Am J Pathol* 2005;167:465–73.
- [10] Steinberger P, Majdic O, Derdak SV, et al. Molecular characterization of human 4lg-B7-H3, a member of the B7 family with four Ig-like domains. *J Immunol* 2004;172:2352–9.
- [11] Chapoval AI, Ni J, Lau JS, et al. B7–H3: a costimulatory molecule for T cell activation and IFN- γ production. *Nat Immunol* 2001;2:269–74.
- [12] Chavin G, Sheinin Y, Crispin PL, et al. Expression of immunosuppressive B7–H3 ligand by hormone-treated prostate cancer tumors and metastases. *Clin Cancer Res* 2009;15:2174–80.
- [13] Lee Y-h, Martin-Orozco N, Zheng P, et al. Inhibition of the B7–H3 immune checkpoint limits tumor growth by enhancing cytotoxic lymphocyte function. *Cell Res* 2017;27:1034–45.
- [14] Luo L, Chapoval AI, Flies DB, et al. B7–H3 enhances tumor immunity in vivo by costimulating rapid clonal expansion of antigen-specific CD8⁺ cytolytic T cells. *J Immunol* 2004;173:5445–50.
- [15] Prasad DV, Nguyen T, Li Z, et al. Murine B7–H3 is a negative regulator of T cells. *J Immunol* 2004;173:2500–6.
- [16] Suh WK, Gajewska BU, Okada H, et al. The B7 family member B7–H3 preferentially down-regulates T helper type 1-mediated immune responses. *Nat Immunol* 2003;4:899–906.
- [17] Wang L, Fraser CC, Kikly K, et al. B7–H3 promotes acute and chronic allograft rejection. *Eur J Immunol* 2005;35:428–38.
- [18] Kreyborg K, Haak S, Murali R, et al. Ablation of B7–H3 but not B7–H4 results in highly increased tumor burden in a murine model of spontaneous prostate cancer. *Cancer Immunol Res* 2015;3:849–54.
- [19] Sun X, Vale M, Leung E, Kanwar JR, Gupta R, Krissansen GW. Mouse B7–H3 induces antitumor immunity. *Gene Ther* 2003;10:1728–34.
- [20] Liu Z, Zhang W, Phillips JB, et al. Immunoregulatory protein B7–H3 regulates cancer stem cell enrichment and drug resistance through MVP-mediated MEK activation. *Oncogene* 2019;38:88–102.
- [21] Zhang T, Jiang B, Zou ST, Liu F, Hua D. Overexpression of B7–H3 augments anti-apoptosis of colorectal cancer cells by Jak2-STAT3. *World J Gastroenterol* 2015;21:1804–13.
- [22] Liu F, Zhang T, Zou S, Jiang B, Hua D. B7H3 promotes cell migration and invasion through the Jak2/Stat3/MMP9 signaling pathway in colorectal cancer. *Mol Med Res* 2015;12:5455–60.

- [23] Du H, Hirabayashi K, Ahn S, et al. Antitumor responses in the absence of toxicity in solid tumors by targeting B7–H3 via chimeric antigen receptor T cells. *Cancer Cell* 2019;35:221–237.e8.
- [24] Scribner JA, Brown JG, Son T, et al. Preclinical development of MGC018, a duocarmycin-based antibody–drug conjugate targeting B7–H3 for solid cancer. *Mol Cancer Ther* 2020;19:2235–44.
- [25] Yamato M, Hasegawa J, Maejima T, et al. DS-7300a, a DNA topoisomerase I inhibitor, DXd-based antibody–drug conjugate targeting B7–H3 exerts potent antitumor activities in preclinical models. *Mol Cancer Ther* 2022;21:635–46.
- [26] Loo D, Alderson RF, Chen FZ, et al. Development of an Fc-enhanced anti–B7–H3 monoclonal antibody with potent antitumor activity. *Clin Cancer Res* 2012;18:3834–45.
- [27] Drago JZ, Modi S, Chandarlapaty S. Unlocking the potential of antibody–drug conjugates for cancer therapy. *Nat Rev Clin Oncol* 2021;18:327–44.
- [28] Cortés J, Kim S-B, Chung W-P, et al. Trastuzumab deruxtecan versus trastuzumab emtansine for breast cancer. *N Engl J Med* 2022;386:1143–54.
- [29] Shitara K, Bang Y-J, Iwasa S, et al. Trastuzumab deruxtecan in previously treated HER2-positive gastric cancer. *N Engl J Med* 2020;382:2419–30.
- [30] Abida W, Cyrta J, Heller G, et al. Genomic correlates of clinical outcome in advanced prostate cancer. *Proc Natl Acad Sci U S A* 2019;116:11428–36.
- [31] Fenor de la Maza MD, Chandran K, Rekowski J, et al. Immune biomarkers in metastatic castration-resistant prostate cancer. *Eur Urol Oncol*. In press. <https://doi.org/10.1016/j.euo.2022.04.004>.
- [32] Rodrigues DN, Rescigno P, Liu D, et al. Immunogenomic analyses associate immunological alterations with mismatch repair defects in prostate cancer. *J Clin Invest* 2018;128:5185.
- [33] Ferraldeschi R, Nava Rodrigues D, Riisnaes R, et al. PTEN protein loss and clinical outcome from castration-resistant prostate cancer treated with abiraterone acetate. *Eur Urol* 2015;67:795–802.
- [34] Sundar R, Miranda S, Rodrigues DN, et al. Ataxia telangiectasia mutated protein loss and benefit from oxaliplatin-based chemotherapy in colorectal cancer. *Clin Colorectal Cancer* 2018;17:280–4.
- [35] Rescigno P, Gurel B, Pereira R, et al. Characterizing CDK12-mutated prostate cancers. *Clin Cancer Res* 2021;27:566–74.
- [36] Mateo J, Carreira S, Sandhu S, et al. DNA-repair defects and olaparib in metastatic prostate cancer. *N Engl J Med* 2015;373:1697–708.
- [37] Gil V, Miranda S, Riisnaes R, et al. HER3 is an actionable target in advanced prostate cancer. *Cancer Res* 2021;81:6207–18.
- [38] Welti J, Sharp A, Yuan W, et al. Targeting bromodomain and extra-terminal (BET) family proteins in castration-resistant prostate cancer (CRPC). *Clin Cancer Res* 2018;24:3149–62.
- [39] Welti J, Sharp A, Brooks N, et al. Targeting the p300/CBP axis in lethal prostate cancer. *Cancer Discov* 2021;11:1118–37.
- [40] He MX, Cuoco MS, Crowdis J, et al. Transcriptional mediators of treatment resistance in lethal prostate cancer. *Nat Med* 2021;27:426–33.
- [41] Chen S, Zhu G, Yang Y, et al. Single-cell analysis reveals transcriptomic remodellings in distinct cell types that contribute to human prostate cancer progression. *Nat Cell Biol* 2021;23:87–98.
- [42] Stuart T, Butler A, Hoffman P, et al. Comprehensive integration of single-cell data. *Cell* 2019;177:1888–1902.e21.
- [43] Aran D, Looney AP, Liu L, et al. Reference-based analysis of lung single-cell sequencing reveals a transitional profibrotic macrophage. *Nat Immunol* 2019;20:163–72.
- [44] Cesano A. nCounter[®] PanCancer immune profiling panel (NanoString Technologies Inc, Seattle, WA). *J Immunother Cancer* 2015;3:42.
- [45] Robinson D, Van Allen EM, Wu YM, et al. Integrative clinical genomics of advanced prostate cancer. *Cell* 2015;162:454.
- [46] Armenia J, Wankowicz SAM, Liu D, et al. The long tail of oncogenic drivers in prostate cancer. *Nat Genet* 2018;50:645–51.
- [47] Carreno BM, Collins M. The B7 family of ligands and its receptors: new pathways for costimulation and inhibition of immune responses. *Annu Rev Immunol* 2002;20:29–53.
- [48] Consortium TU. UniProt: a worldwide hub of protein knowledge. *Nucl Acids Res* 2018;47:D506–15.
- [49] Bonk S, Tasdelen P, Kluth M, et al. High B7–H3 expression is linked to increased risk of prostate cancer progression. *Pathol Int* 2020;70:733–42.
- [50] Parker AS, Heckman MG, Sheinin Y, et al. Evaluation of B7–H3 expression as a biomarker of biochemical recurrence after salvage radiation therapy for recurrent prostate cancer. *Int J Radiat Oncol Biol Phys* 2011;79:1343–9.
- [51] Epstein JI, Amin MB, Beltran H, et al. Proposed morphologic classification of prostate cancer with neuroendocrine differentiation. *Am J Surg Pathol* 2014;38:756–67.
- [52] Sato H, Niimi A, Yasuhara T, et al. DNA double-strand break repair pathway regulates PD-L1 expression in cancer cells. *Nat Commun* 2017;8:1751.
- [53] Kontos F, Michelakos T, Kurokawa T, et al. B7–H3: an attractive target for antibody-based immunotherapy. *Clin Cancer Res* 2021;27:1227–35.
- [54] Flem-Karlsen K, Tekle C, Andersson Y, Flatmark K, Fodstad O, Nunes-Xavier CE. Immunoregulatory protein B7–H3 promotes growth and decreases sensitivity to therapy in metastatic melanoma cells. *Pigment Cell Melanoma Res* 2017;30:467–76.
- [55] Hofmeyer KA, Ray A, Zang X. The contrasting role of B7–H3. *Proc Natl Acad Sci U S A* 2008;105:10277–8.
- [56] Brady L, Kriner M, Coleman I, et al. Inter- and intra-tumor heterogeneity of metastatic prostate cancer determined by digital spatial gene expression profiling. *Nat Commun* 2021;12:1426.
- [57] Amori G, Sugawara E, Shigematsu Y, et al. Tumor B7–H3 expression in diagnostic biopsy specimens and survival in patients with metastatic prostate cancer. *Prostate Cancer Prostatic Dis* 2021;24:767–74.
- [58] Dong P, Xiong Y, Yue J, Hanley SJB, Watari H. B7H3 as a promoter of metastasis and promising therapeutic target. *Front Oncol* 2018;8:264.
- [59] Ogitani Y, Hagihara K, Oitate M, Naito H, Agatsuma T. Bystander killing effect of DS-8201a, a novel anti-human epidermal growth factor receptor 2 antibody–drug conjugate, in tumors with human epidermal growth factor receptor 2 heterogeneity. *Cancer Sci* 2016;107:1039–46.
- [60] Deng L, Liang H, Burnette B, et al. Irradiation and anti-PD-L1 treatment synergistically promote antitumor immunity in mice. *J Clin Invest* 2014;124:687–95.
- [61] Rosenbaum MW, Bledsoe JR, Morales-Oyarvide V, Huynh TG, Mino-Kenudson M. PD-L1 expression in colorectal cancer is associated with microsatellite instability, BRAF mutation, medullary morphology and cytotoxic tumor-infiltrating lymphocytes. *Mod Pathol* 2016;29:1104–12.
- [62] Antonarakis ES, Piulats JM, Gross-Goupil M, et al. Pembrolizumab for treatment-refractory metastatic castration-resistant prostate cancer: multicohort, open-label phase II KEYNOTE-199 study. *J Clin Oncol* 2020;38:395–405.
- [63] Jenzer M, Keß P, Nientiedt C, et al. The BRCA2 mutation status shapes the immune phenotype of prostate cancer. *Cancer Immunol Immunother* 2019;68:1621–33.
- [64] Mendes AA, Lu J, Kaur HB, et al. Association of B7–H3 expression with racial ancestry, immune cell density, and androgen receptor activation in prostate cancer. *Cancer* 2022;128:2269–80.
- [65] Jänne PA, Baik C, Su W-C, et al. Efficacy and safety of patritumab deruxtecan (HER3-DXd) in EGFR inhibitor-resistant, EGFR-mutated non-small cell lung cancer. *Cancer Discov* 2022;12:74–89.
- [66] Modi S, Saura C, Yamashita T, et al. Trastuzumab deruxtecan in previously treated HER2-positive breast cancer. *N Engl J Med* 2020;382:610–21.
- [67] Pommier Y. DNA topoisomerase I inhibitors: chemistry, biology, and interfacial inhibition. *Chem Rev* 2009;109:2894–902.
- [68] Coussy F, El-Botty R, Château-Joubert S, et al. BRCAness, SLFN11, and RB1 loss predict response to topoisomerase I inhibitors in triple-negative breast cancers. *Sci Transl Med* 2020;12:eaax2625.
- [69] Tomicic MT, Kaina B. Topoisomerase degradation, DSB repair, p53 and IAPs in cancer cell resistance to camptothecin-like topoisomerase I inhibitors. *Biochim Biophys Acta* 2013;1835:11–27.
- [70] Stein GH, Drullinger LF, Soulard A, Dulic V. Differential roles for cyclin-dependent kinase inhibitors p21 and p16 in the mechanisms of senescence and differentiation in human fibroblasts. *Mol Cell Biol* 1999;19:2109–17.